Calibration functions in approximate simulations of equilibrium adsorption characteristics

Yu. K. Tovbin, A. B. Rabinovich, and E. V. Votyakov*

State Research Center of the Russian Federation "L. Ya. Karpov Institute of Physical Chemistry," 10 ul. Vorontsovo Pole, 103064 Moscow, Russian Federation. Fax: +7 (095) 975 2450. E-mail: tovbin@cc.nifhi.ac.ru

The calibration functions based on an information on exact solutions were used for the uniform and nonuniform systems to enhance the accuracy of phase diagram calculations using approximate cluster methods. This approach was used for the description of adsorption on uniform surfaces (two-dimensional system) and in porous sorbents (three-dimensional system). The quasichemical approximation and accurate information on the regions of critical points in uniform lattices were used. The current state of phase diagram simulations in porous systems is discussed.

Key words: phase diagram, slit-like pore, adsorption, isotherm, lattice model, quasichemical approximation, argon.

Equilibrium thermodynamic characteristics of adsorption (isotherms, heats, thermal capacities) have been experimentally studied in wide ranges of temperatures of an adsorption system and pressures of adsorbed substances.[1—3] Effects of interparticle interaction become significant in regions of medium and high coverages. These effects determine the aggregate states and type of ordered structures of condensed phases of the adsorbate and influence the concentration relationships for adsorption characteristics.[4] Exact solutions for the description of adsorption are known only for one-dimensional ($d = 1$, d is the dimensionality of the system), uniform, a series of nonuniform, and several particular cases of two-dimensional uniform lattices.[5—7] This stimulated the active development of the approximate[1,4,6] and numerical (Monte Carlo and molecular dynamics methods)[8—11] methods for calculation of equilibrium characteristics. Numerical methods describe in detail molecular distributions and provide an almost accurate (from the statistical point of view) result for $d = 2$ and 3. However, they require the computation time two—five orders of magnitude longer than the approximate methods based on the lattice-gas model.[4—7] Therefore, different authors[12—14] repeatedly quested for modifications of approximate simulations, which would improve the accuracy of description of adsorption characteristics without a substantial increase in the computation time. These modifications are based on the use of exact values of critical parameters to improve the quasichemical approximation (QCA).

The quasichemical approximation has several advantages: (1) it allows fast computations, (2) reflects effects of direct correlations, *i.e.*, takes into account the influence of direct interactions between particles on the character of their distribution (this approximation ignores effects of indirect correlations when particles are remote at distances longer than the potential interaction radius), (3) gives accurate results in the region of weak and strong interactions, and (4) provides a qualitatively valid description in the critical region (better than the mean field approximation gives).[4,6,14] Using additional data on exact solutions, we can plot a calibration (fitting) function, which provides the agreement of approximate calculations with exact solutions in the region of their existence and thus improves substantially the accuracy of calculations in the whole region of the phase diagram.

As mentioned previously,[14] the calibration function can be introduced into the QCA equations through either the effective parameters of lateral interaction or the entropy component of the free energy. In both variants, the calibration function depends on the temperature T and the coverage of the surface with the adsorbate θ ($\theta = N_A/N$, where N_A is the number of adsorbed particles, each occupying one site of the surface, and N is the number of sites per unit surface). The calibration functions should provide the transition of equations of the calibrated QCA (CQCA) into equations of the normal QCA in the region of high ($\theta \to 1$) and low ($\theta \to 0$) coverages and for low ($\beta\varepsilon \to \infty$) and high ($\beta\varepsilon \to 0$) temperatures ($\beta = (RT)^{-1}$, R is the universal gas constant, and ε is the parameter of lateral interaction between the nearest neighbors), and their parameters should satisfy the equations describing the position of the critical point $d\ln P/d\theta|_T = d^2\ln P/d\theta^2|_T = 0$ (P is the adsorbate pressure). In the first case, the calibration function enters

Published in Russian in *Izvestiya Akademii Nauk. Seriya Khimicheskaya,* No. 9, pp. 1531—1538, September, 2002.

1066-5285/02/5109-1667 $27.00

the equation for pair functions, and all thermodynamic characteristics in the CQCA are calculated by standard expressions.[4] However, in this variant the introduction of the calibration function can change the symmetry (or antisymmetry) of the calculated characteristics with respect to the coverage $\theta = 1/2$.[14]

In this work we used the second method of introduction of calibration functions, namely, through the entropy component of the free energy under the conditions of retention of the symmetry properties. This condition is normal for the lattice model.[4–7] (Remind that the symmetry property is that the statistical weight of configuration of particles remains unchanged when occupied sites are replaced by free sites, and *vice versa*. In particular, this appears as the symmetry of the condensation curve for the uniform lattice with $d = 2$ and 3 with respect to $\theta = 1/2$.) First let us consider the case of a uniform surface and then the general case of a nonuniform lattice in relation to the porous system (argon—slit-like carbon pore) in which the nonuniform over the pore cross-section distribution of an adsorbate is realized. The study of the phase diagrams in porous systems is of independent significance, and the use of the calibration functions suggests the current state of the problem under question, in particular, the existence of phase transitions of an adsorbate in near-surface layers of slit-like pores. (Further we will restrict our consideration by allowance for the interaction of only z nearest neighbors.)

Uniform lattice

Let us present the calibration equation for the adsorption isotherm in the form

$$aP = [\theta/(1-\theta)]^{1+g\Lambda}, \qquad (1)$$

$$\Lambda = (1+xt)^z, \qquad x = \exp(-\beta\varepsilon) - 1,$$

$$t = \theta_{AA}/\theta_A = 1 - 2(1-\theta)/(1+\delta),$$

$$\delta = \{1 + 4\theta(1-\theta)[\exp(\beta\varepsilon) - 1]\}^{0.5},$$

where a is the Langmuir constant; g is the calibration function modifying the entropy component of the free energy; Λ is the function taking into account lateral interactions between the adsorbate molecules, at $g = 0$ we have the normal CQA; $t = \theta_{AA}/\theta_A$ ($\theta_A \equiv \theta$), the following relations are valid for the pair functions: $\theta_{AA}\theta_{vv} = \theta_{Av}^2\exp(\beta\varepsilon)$, where θ_{ij} are the probabilities that a pair of particles ij occurs alongside (i, j = A, v, A is adsorbate, and v is vacancy), $\theta_{ii} + \theta_{ij} = \theta_i$, and $\theta_A + \theta_v = 1$. The relation of θ to P (1) determines all other equilibrium adsorption characteristics.[4]

In the general case, the problem of plotting a calibration function is ambiguous, and it is reasonable to take into account a particular character of differences between the exact and approximate solutions. For a uniform lattice, the exact and approximate (in the QCA) θ values in the critical point (θ_c) coincide; therefore, it is enough to consider the case when the calibration function is temperature-dependent and independent of θ. This automatically satisfies the second condition for the critical parameters $d^2\ln P/d\theta^2|_T = 0$.

The critical temperature is determined by the condition $d\ln P/d\theta|_T = 0$; therefore, after differentiating Eq. (1) with respect to coverage θ we have

$$\frac{d\ln P}{d\theta} = \frac{1+g(\tau)}{\theta(1-\theta)} + \frac{d\ln\Lambda}{d\theta}, \qquad (2)$$

where $\tau = (\beta\varepsilon)_{exact}/(\beta\varepsilon)$ is the reduced temperature; $(\beta\varepsilon)_{exact}$ corresponds to the exact value of critical temperature in the model considered. Then the critical value of the reduced temperature in the CQA will be designated as $\tau_c = (\beta\varepsilon)_{exact}/(\beta\varepsilon)_c^{QCA}$.

For the CQA modification, the $g(\tau)$ function should differ from zero in the vicinity of the $(1, \tau_c)$ interval and provide the uniqueness of solution $d\ln P/d\theta = 0$ at $\tau = 1$ and the critical value of coverage $\theta_c = 0.5$.

According to these demands for function $g(\tau)$ with allowance for Eq. (2), we construct the following equation:

$$g(\tau) = \left[a(\tau) - 1 - \theta_c(1-\theta_c)\frac{d\ln\Lambda}{d\theta}\bigg|_{\theta=0.5}\right]b(\tau), \qquad (3)$$

where function $a(\tau)$ should be equal to zero at $\tau = 1$, and function $b(\tau)$ should be equal to unity at $\tau = 1$ and $\tau = \tau_c$ in order to exceed unity within the interval and tend to zero outside it, and both functions $a(\tau)$ and $b(\tau)$ tend to zero at $\tau \to \infty$. The $b(\tau)$ function determines the region of phase diagram in which the calibration function "operates." The $a(\tau)$ and $b(\tau)$ functions satisfy the requirements listed as containing the minimum number of parameters and can be presented in the form

$$a(\tau) = (1-\tau)\exp(1-\tau),$$

$$b(\tau) = [1 + (D-1)/\Delta]^m/[1 + (D-\tau)/\Delta]^m. \qquad (4)$$

Here the parameter $D = (1 + \tau_c)/2$ determines the dimension of the region $(1, \tau_c)$ in which the $b(\tau)$ function remarkably differs from unity (and, hence, the $g(\tau)$ function differs from zero), and the m and Δ parameters determine the curvature of the coexistence curve in the critical region.

It follows from Eqs. (3) and (4) that the calculation of the calibration function requires exact values of the critical parameters (θ_c and T_c or $\beta_c\varepsilon$) and the temperature relationship $d\ln\Lambda/d\theta$ at the unchanged density θ_c, which is obtained from the preliminary calculation of

the phase diagram in the QCA. The exact values of critical parameters can be known from either analytical solutions (which is possible only in rare cases[5]) or numerical calculations by the Monte Carlo or molecular dynamics methods. In the general case, one has to find the parameters m, Δ, and D of calibration function (4) from comparison with the exact solutions. The numerical analysis performed for the coexistence curves demonstrated the following simplifications: (1) for plotting function $b(\tau)$ parameter m should take even values (2, 4, 6, ...); however, it turned out that $m = 2$ is enough; (2) parameter D at the unchanged θ_c density can be expressed as

$$D = (1 + T_c^{QCA}/T_c^{exact})/2, \; m = 2, \qquad (5)$$

i.e., the knowledge of the critical temperature in the exact and approximate solutions is sufficient. This allows an additional decrease in the number of parameters for the calibration curve. The single parameter of the $g(\tau)$ function is Δ, which can be related to the critical parameters.[15]

It is well known that the two-dimensional system with $z = 4$ has the exact Onsager solution[16,17] for which $(\beta\varepsilon)_c^{exact} = 1.76$, while for the QCA $(\beta\varepsilon)_c^{QCA} = 1.38$. This example demonstrates the influence of the calibration curve on the phase diagram pattern when the normal and calibrated QCA are used. The comparison of the QCA curve (Fig. 1, curve *1*) and exact curve[6,16,17] (see Fig. 1, curve *3*) shows that the QCA curve satisfactorily corresponds to the accurate result at low temperatures (low and high coverages of the lattice) but remarkably differs from it at medium coverages. Curve *2* (see Fig. 1) corresponds to the CQCA at $\Delta = 0.06$, and curve *4* refers to re-scaled curve *1* in the same figure when $(\beta\varepsilon)_c^{QCA} = 1.38$ is accepted as unity: the points in curve *4* were obtained from the points in curve *1* by dividing all ordinate values by 1.38. This approach (plotting coexistence curves in the dimensionless coordinates T/T_c—θ to compare experimental data and results of approximate calculation methods) is standard and allows a good description of various experimental data for vapor-liquid systems.[18—21] The latter fact can be theoretically substantiated in the framework of the principle of corresponding states, which is widely used in theory to describe experimental data (phase diagrams, viscosities, second virial coefficients, *etc.*).[19]

At the temperature $2T_c$ the exact adsorption isotherm[22] (Fig. 2, points) and curve *2* calculated in the QCA (since at this temperature the isotherms in the QCA and CQCA coincide) are sufficiently close to each other. The isotherm (curve *1*) for the critical temperature T_c is presented in Fig. 2 for comparison.

Thus, the introduction of the calibration function improves considerably the traditional QCA and allows calculation of the equilibrium adsorption characteristics with a high accuracy in the whole region of the phase diagram. The calibration function introduces a refinement similar to the account of large-scale fluctuations in the scaling theory of phase transitions[15] (which is absent from the QCA itself) in the vicinity of the critical region in addition to local correlations in the QCA. Therefore, the main properties of the calibration function $g(\tau)$ established for uniform systems should be valid for nonuniform systems if the dimensions of regions of nonuniformities are small. The latter means that the system contains no macroscopic regions different in properties. In particular, such a surface has one phase transition of the adsorbate of the vapor—liquid type.[4,23] Due to the

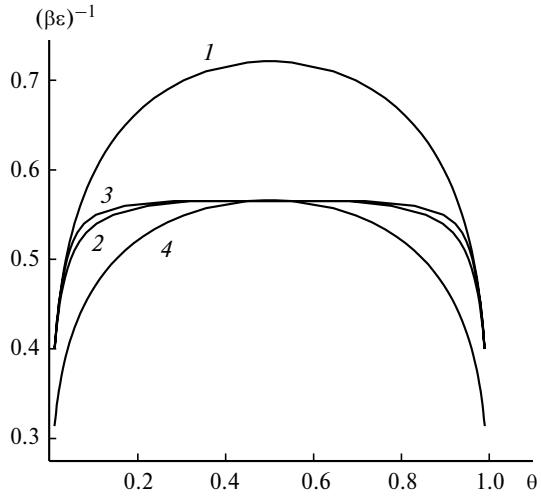

Fig. 1. Phase diagram for the square-planar lattice calculated in the traditional (*1*) and calibrated QCA (*2*) and the exact solution (*3*). Curve *4* corresponds to corrected curve *1* presented in the dimensionless coordinates T/T_c—θ.

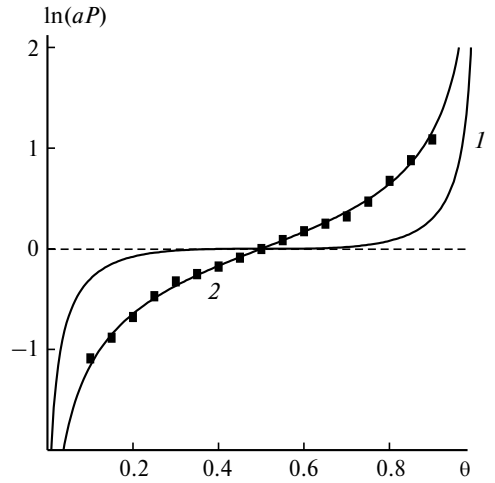

Fig. 2. Adsorption isotherms at the critical temperature T_c (*1*) and temperature $2T_c$ (*2*) calculated in the CQCA. Points mark the region of the exact isotherm[22] at $2T_c$ in the region of medium coverage.

foregoing, parameters D, m, and Δ must be virtually constant (or slightly varying) and can be determined from the analysis of uniform systems.

Nonuniform systems

The direct generalization of Eq. (1) for local isotherms based on the model,[4,7,24] which takes into account interactions of the nearest neighbors in the quasichemical approximation, is written for nonuniform lattices as

$$\theta(P) = \sum_{f=1}^{N} \theta_f(P)/N,$$

$$a_f P = [\theta_f/(1-\theta_f)]^{1+g} \Lambda_f,$$

$$\Lambda_f = \prod_{h \in z} (1 + t_{fh} x_{fh}), \qquad (6)$$

where θ_f is the coverage of site f, $1 \le f \le N$, N is the number of units of a lattice, and a_f is local Henry´s constant for site f with the energy of adsorbate—adsorbent interaction Q_f. Index h corresponds to the sites arranged around central site f. Formula (6) assumes the detailed description of coverages of all sites of a nonuniform lattice. The expressions for the conditional probabilities t_{fh} of the location of a neighboring particle in site h with respect to the "central" particle located in site f in formula (6) have the following form:

$$t_{fh} = \theta_{fh}^{AA}/\theta_f,$$

where θ_{fh}^{AA} is the probability that two particles occur in the neighboring sites f and h

$$t_{fh} = 2\theta_h/(\delta_{fh} + b_{fh}), \qquad \delta_{fh}(r) = 1 + x_{fh}(1 - \theta_f - \theta_h),$$

$$x_{fh} = \exp(-\beta\varepsilon_{fh}) - 1, \qquad b_{fh} = (\delta_{fh}^2 + 4x_{fh}\theta_f\theta_h)^{0.5}.$$

Additionally, the following normalization relations were taken into account:

$$\theta_{fh}^{AA}(r) + \theta_{fh}^{Av}(r) = \theta_f \equiv \theta_f^{A},$$

$$\theta_{fh}^{vA}(r) + \theta_{fh}^{vv}(r) = \theta_f^{v} = 1 - \theta_f,$$

$$\theta_f^{A} + \theta_f^{v} = 1.$$

The calibration function g in formula (6) has the same structure as that in formulas (3) and (4). It is also obtained from the condition $d\ln P/d\theta = 0$, which gives

$$\frac{1+g}{\theta_f(1-\theta_f)}\frac{d\theta_f}{d\theta} + \frac{d\ln\Lambda_f}{d\theta} = 0\,. \qquad (7)$$

Expressing the derivative

$$d\theta_f/d\theta = \theta_f(1-\theta_f)/(1+g) + d\ln\Lambda_f/d\theta$$

and using the normalization conditions $\sum_{f=1}^{N} \theta_f = N\theta$ and $\sum_{f=1}^{N} d\theta_f/d\theta = N$, we get the following generalization of formula (3):

$$g(\tau) = \left[a(\tau) - 1 - \sum_f \frac{\theta_{fc}(1-\theta_{fc})}{N} \left.\frac{d\ln\Lambda_f}{d\theta}\right|_{\theta_c}\right] b(\tau), \qquad (8)$$

where θ_{fc} is the local coverage of site f at the macroscopic density of the adsorbate in the critical point θ_c, and the $a(\tau)$ and $b(\tau)$ functions are specified by formulas (4) and (5).

Instead of the discrete description of the nonuniform surface over each site, one can use the averaged description using the distribution functions of adsorption centers F_q ($\sum_q F_q = 1$) over local Henry´s constants a_q, where $1 \le q \le t$, t is the number of types of sites on the nonuniform surface. In this case, the equation of local isotherm has the form

$$\theta(P) = \sum_{q=1}^{t} F_q \theta_q(P),$$

$$a_q P = [\theta_q/(1-\theta_q)]^{1+g} \Lambda_q,$$

$$\Lambda_q = \left(1 + \sum_p d_{dp} t_{dp} x_{dp}\right)^z, \qquad (6a)$$

where the surface structure is specified by the averaged manner[4] through functions d_{qp}, $1 \le p \le t$. Then formula (8) takes the form

$$g(\tau) = \left[a(\tau) - 1 - \sum_q F_q \theta_{qc}(1-\theta_{qc}) \left.\frac{d\ln\Lambda_q}{d\theta}\right|_{\theta_c}\right] b(\tau), \qquad (8a)$$

where θ_{qc} is the local coverage of site q at the macroscopic coverage θ_c of the surface with an adsorbate in the critical point.

The macroscopic character of the cooperative (rather than local) behavior of interacting particles in the vicinity of the critical point is reflected by the fact that function g in formulas (8) is independent of indices f or q. Meanwhile, it is known for nonuniform systems that the number of phase transitions depends on the composition and structure of two- and three-dimensional lattices.[4] In particular, in the case of the same order of all F_q magnitudes ($1 \le q \le t$), the number of the first order phase transitions was established[23,25,26] to vary from 1 to t, depending on the character of arrangement of adsorp-

tion sites of different types (*i.e.*, on functions d_{qp} at constant F_q values). Unity corresponds to the case when all lattice sites of different types form a periodically repeated "pattern" and all of them are involved in the formation of the dense and low-density phases. Number t corresponds to the case when each region consisting of the same centers forms its dense and low-density phases. Therefore, nonuniform lattices contain a set of pairs of the critical densities θ_c^k and temperatures T_c^k, where the number of phase transitions is $1 \le k \le K(F_q,d_{qp})$, and $K(F_q,d_{qp})$ is the number of phase transitions for the particular unchanged values of functions F_q and d_{qp} describing the composition and structure of a nonuniform lattice.

When calibration functions (8) are used, one accepts that the regions of existence of different phase transitions are described in the QCA rather accurately and for each phase transition functions (8) depend on the temperature only, like for uniform lattices. The physical basis for this assertion is the fact that at low temperatures the QCA provides an almost exact solution of the problem on the molecular distribution over different sites.[4] For each phase transition, critical coverages θ_c^k are determined from the preliminary calculation of the phase diagrams in the QCA, and the same concerns local densities θ_{qc}, critical temperatures T_c^k(QCA), and derivatives $d\ln\Lambda_q/d\theta$ at the unchanged θ_c^k. These values are further used in calibration functions g_k, $1 \le k \le K(F_q,d_{qp})$. Additionally, one has to know the exact values of critical temperatures $(T_c^k)^{exact}$ or plot estimates for them.

In the absence of independent data on exact solutions for all phase transitions of a nonuniform system, such estimates can be obtained from available data on exact ($T_c^{exact}(d)$) and approximate ($T_c^{QCA}(d)$) critical temperatures in uniform lattices with dimensionality d using the corresponding corrections Δ_d ($d = 2$ or 3):

$$\Delta_d = T_c^{exact}(d) - T_c^{QCA}(d). \quad (9)$$

As for θ_c^k, the introduction of corrections Δ_d is based on the fact that the QCA rather accurately reflects a change in the critical temperature on going from uniform to nonuniform systems. Therefore, a uniform system, for which an accurate information is available, can always be chosen, and corrections Δ_d can be found from the changes in physical properties (Henry´s constants, composition, and structure) of a nonuniform surface with respect to the chosen uniform surface. Below we demonstrate the use of such corrections in analysis of the phase diagrams in slit-like pores.

Slit-like pores

As an example of using Eqs. (8a) and (9), let us consider the adsorption of spherical particles in slit-like pores (three-dimensional system) with uniform walls (calibration functions are plotted from the data on phase diagrams for two- and three-dimensional uniform systems). A slit-like pore is considered to be formed by two infinite solid plates parallel to the xz plane (periodical boundary conditions are imposed on the system in the directions and x and z). The potential for the adsorbate interaction with the wall was calculated as the sum $U(y) + U(H - y)$, where $U(y)$ is the model potential of adsorbate—wall interaction, y is the distance to the wall, and H is the pore width. The pore space is divided into particular monolayers, and then each layer is separated into unit volumes (units) $v_0 = \lambda^3$ (λ is the lattice constant) equal to the particle size. Each monolayer consists of equivalent units with the same adsorption characteristics, including the same energy of adsorbate—adsorbent interaction Q_q ($1 \le q \le t$, where t is the number of types of monolayers in a slit-like pore[27—30]), and then $F_q = 1/H$. For a slit-like pore, in the case of uniform walls, due to symmetrical adsorbate distribution, set (6a) can be solved not only for the whole pore width H but only for the region before the central layer, taking into account that for the central layer with number t the properties of units located in the adjacent layers h differ for the even and odd numbers of the layers in the pore H.[27—30] The equilibrium distribution of particles over units of different types was found from the set of equations (6a) by the Newtonian iteration method. The accuracy of the solution of this set is ~0.1%.

A lattice with the number of the nearest neighbors $z = 6$ will be used as the main lattice structure because, as it has been repeatedly mentioned,[4,6,21,31] this structure gives the best agreement of the critical parameters and experimental data for the bulk fluids. The results of calculations of the phase diagrams are presented below in the coordinates $(\beta\varepsilon)^{-1}$—θ^*, where $\theta^* = \theta(\sigma/\lambda)^3$ is the numerical density of the adsorbate when the volume of the solid sphere of a particle is taken as the unit volume. (The θ^* units are normally used in numerical methods of investigations.[8—11]) For a rigid (incompressible) lattice $\theta^* = \theta/1.41$ because the lattice constant λ is related to the parameter of the Lennard-Jones potential for adsorbate molecules as $\lambda = 1.12\sigma_{AA}$. The limiting θ^* value in these calculations is ~0.71. The following accurate data for two- and three-dimensional lattices[13,17]: were used to calculate Δ_2 and Δ_3: $(\beta\varepsilon)_c^{exact} = 1.76$ for $z = 4$, $d = 2$ and $(\beta\varepsilon)_c^{exact} = 0.886$ for $z = 6$, $d = 3$. The condensation curves for the three-dimensional uniform lattice with $z = 6$ in the CQCA and QCA is shown in Fig. 3 in the coordinates $(\beta\varepsilon)^{-1}$—θ. The parameters D and m from formula (5) and $\Delta = 0.06$ were used (as well as those for the slit-like pores, see below).

The phase diagrams for the adsorption of Ar atoms in a slit-like carbon pore with a width of 11 monolayers in the QCA and CQCA are presented in Fig. 4. The molecular parameters of the system correspond to the pub-

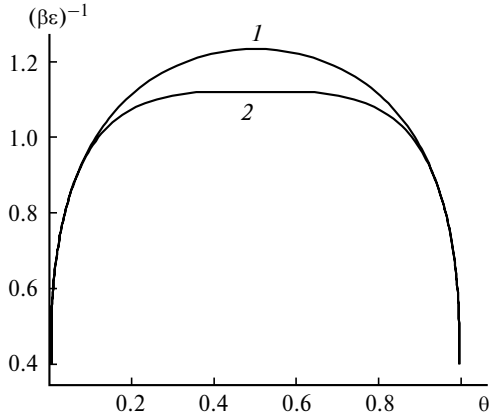

Fig. 3. Phase diagram for the cubic lattice calculated in the traditional (*1*) and calibrated QCA (*2*).

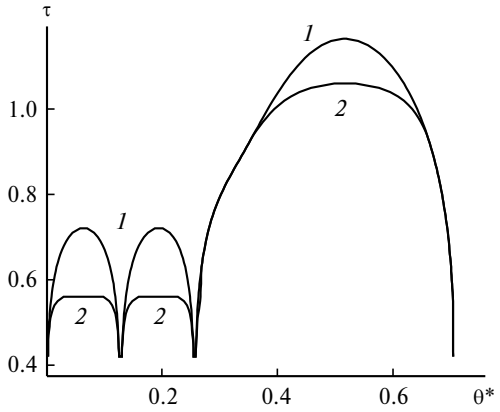

Fig. 4. Phase diagrams of Ar in a slit-like pore of carbon in the QCA (*1*) and CQCA (*2*); $Q_1 = 9.246\varepsilon$, $\varepsilon = 0.238$ kcal mol^{-1}, $Q_2 = Q_1/8$, $z = 6$, $H = 11$.

lished data[32]: $Q_1 = 9.24\varepsilon$, $Q_2 = Q_1/8$, the other $Q_{q>2} = 0$; $\varepsilon = 0.238$ kcal mol^{-1} is the parameter of interaction between Ar atoms. The initial phase diagram in the QCA consists of three domes. The first two domes refer to the first two near-surface layers, and the third dome refers to the rest of the pore including its core (beginning from the third monolayer, the numeration starts from the pore walls).

It is well known[27,28,33—36] that allowance for the restricted space in pores introduces substantial changes in the conditions of realization of phase transitions compared to unrestricted systems. When choosing calibration functions on the basis of the initial phase diagram in the QCA, we took into account the above specific feature of different phase transitions: they were considered as two-dimensional in each near-surface layer, and the phase transition for the core of a pore was considered as a three-dimensional phase transition. To reflect these factors, we accepted that the "exact" critical densities θ_c^k for each transition correspond to the calculation of "pure" QCA (as mentioned above), and the following values were specified as exact critical temperatures in the near-surface layers:

$$T_c^k = \begin{cases} T_c\,(d = 2), & k = 1, \\ T_c^2(\mathrm{QCA}) + \Delta_2, & k = 2, \\ T_c^3(\mathrm{QCA}) + \Delta_3, & k = 3. \end{cases} \qquad (10)$$

Here the Δ_d values were determined using expression (9). Equations (10) mean that (1) the exact temperature value for a two-dimensional unrestricted system ($d = 2$) was used for the surface layer $k = 1$ because there is a complete correspondence between the surface layer in a pore and two-dimensional lattice (except for the case of $H = 2$ for which a uniform lattice system with the number of the nearest neighbors equal to five is realized in a pore, which also retains this relation); (2) deviations of the T_c^2 value in the second layer ($k = 2$) from the conditions of phase transition in the first layer are caused by the influence of the surface potential rather than the cooperative behavior of molecules (and analogously for the subsequent near-wall layers if they are present in the system); (3) similarly, deviations of the T_c^3 value from the conditions of phase transition in the bulk phase are also caused by the influence of the surface potential rather than the cooperative behavior of molecules.

The calibration function substantially decreases the critical temperature of phase transitions (see Fig. 4), and in relative fractions this decrease is stronger for the near-surface layers than for the core of a pore. All domes become more flattened. In both the initial QCA and CQCA, the domes for both near-surface layers are rather close to each other.

The influence of the calibration function for a slit-like pore with the same width but a weak adsorbent—adsorbate interaction is shown in Fig. 5. It is not advantageous for molecules to form a two-dimensional flatten structure near the pore wall, and they form clusters (associates) of

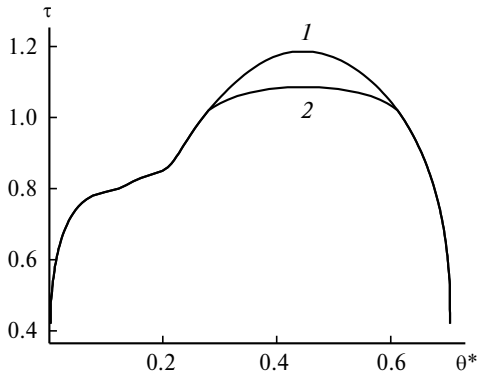

Fig. 5. Calibrated phase diagrams of Ar in slit-like pores with a width of 11 monolayers for $Q_1 = 1.0\varepsilon$ (*1*) and $Q_2 = Q_1/8$ (*2*); $z = 6$.

a new phase in several adjacent layers. In this situation, the near-surface domes are absent and only one dome referred to the volume filling of a pore is realized. As earlier, in the CQCA the dome is flattened, and the critical temperature decreases.

Near-surface phases

Phase diagrams are the main equilibrium characteristics, and one needs knowing them to interpret all equilibrium and dynamic properties of porous systems. The experimental determination of phase diagrams for porous systems is very difficult and, hence, their theoretical prediction is of special significance.[37,38]

Various theoretical methods (*viz.*, Monte Carlo, molecular dynamics, density functional, and lattice-gas model) brought about approximately the same results for the properties of the central dome. This dome shifts to higher densities in the case of a stronger bonding of the adsorbate with the support than the bond between the adsorbate molecules, as it takes place for the adsorption of inert gases on carbon sorbents or silica gel. For example, a comparison of the calculations using the lattice-gas model ("normal" QCA) and molecular dynamics method for Ar atoms in carbon pores showed[29] that when the reduced coordinates τ—θ^* are used ($\tau = T/T_c$(bulk), an analog of curve *4* in Fig. 1), a quantitative agreement is observed (the difference between the critical temperatures calculated in the lattice model and using the accurate numerical methods is ~6%). Similar quantitative agreement was obtained[30] when the influence of the pore width on the character of displacement of the critical point was studied by the lattice-gas model and Monte Carlo method.

However, there is a substantial discrepancy between the results concerning the existence of near-surface phases obtained by the numerical methods and the lattice-gas model. These near-surface phases are formed by the layer-by-layer filling of adsorbents in the case of a strong attraction of the adsorbate, as it occurs in the above systems (inert gases in carbon adsorbents or silica gel).

The introduction of calibration functions allows one to do away with indirect comparison of the phase diagrams through the reduced temperature coordinate and to compare directly the results of numerical experiments and the lattice-gas model in the CQCA. The influence of the wall potential on the phase diagram for the above-considered model of a pore with a width of 11 monolayers is presented in Fig. 6. The layer-by-layer condensation is distinctly observed for different wall potentials exceeding interactions between Ar molecules. These curves show that a more accurate calculation using an additional information on exact solutions for two- and three-dimensional systems confirms completely the qualitative conclusion obtained previously in the QCA that the near-wall phases exist and accounts for their absence from numerical procedures.

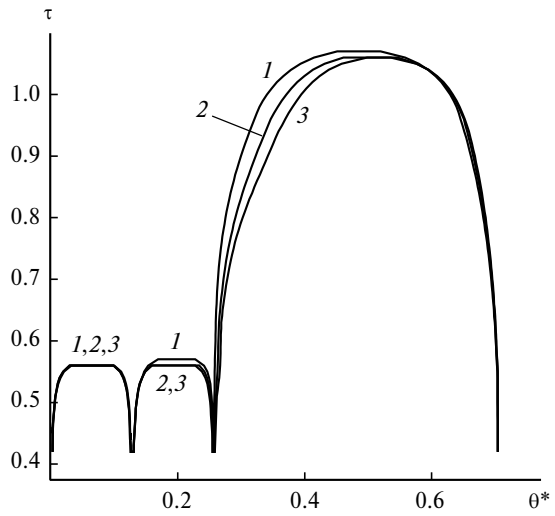

Fig. 6. Calibrated phase diagrams of Ar in slit-like pores with a width of 11 monolayers for $Q_1 = 9.246\varepsilon$ (*1*), 4.0ε (*2*), and 2.0ε (*3*), $Q_2 = Q_1/8$, $z = 6$.

As a rule, studies using numerical procedures were performed in the region $0.60—0.65 < \tau \leq 1$. With a decrease in τ, the time of calculations increases dramatically and the accuracy of results decreases. It is seen in Fig. 6 that the temperatures corresponding to $\tau < 0.5$ should be considered for studying the near-wall phases but this region is poorly accessible for numerical procedures.

The estimates presented in this work were obtained for the simplest variant of allowance for the interaction of only the nearest neighbors with the potential corresponding to Ar atoms. However, a comparison with analogous data[38] shows that the results are valid when further contributions to the interaction potential are taken into account and concern all spherical particles (*viz.*, inert gases, molecules of the CA_4 type, where A is the H or halogen atom) in both slit-like and cylindrical pores. For narrow pores with the width from 1 to 7 nm, contributions from the near-wall and central domes to the phase diagrams have the same order. Evidently, with an increase in the pore width, the contribution of the central dome to the phase diagrams increases and that of the near-surface layers decreases (although the near-surface layers remain). For broad mesopores (≥20 nm), the contributions of the near-wall domes can be neglected.

Thus, the procedure of calibration functions in the QCA (in the lattice-gas model) makes it possible to obtain more reliable data and verify calculations performed by numerical methods because this procedure is based on an accurate information.

This work was supported by the INTAS (Grant 00-505).

References

1. N. N. Avgul´, A. V. Kiselev, and D. P. Poshkus, *Adsorbtsiya gazov i parov na odnorodnykh poverkhnostyakh* [*Adsorption on Gases and Vapors on Uniform Surfaces*], Khimiya, Moscow, 1975, 384 pp. (in Russian).
2. M. W. Roberts and C. S. Mckee, *Chemistry of the Metal—Gas Interface*, Clarendon Press, Oxford, 1978.
3. *Experimental Methods in Catalytic Research*, Ed. R. B. Anderson, Academic Press, New York—London, 1968.
4. Yu. K. Tovbin, *Teoriya fiziko-khimicheskikh protsesov na granitse gaz—tverdoe telo* [*The Theory of Physicochemical Processes at the Gas—Solid Interface*], Nauka, Moscow, 1990, 288 pp. (in Russian).
5. R. J. Baxter, *Exactly Solved Model in Statistical Mechanics*, Academic Press, London, 1982.
6. T. L. Hill, *Statistical Mechanics. Principles and Selected Applications*, McGraw-Hill Book Comp. Inc., New York, 1956.
7. Yu. K. Tovbin, *Khim. Fiz.*, 1996, **15**, 75 [*Chem. Phys. Reports*, 1996, **15**, No. 1 (Engl. Transl.)]; *Zh. Fiz. Khim.*, 1996, **70**, 700 [*Russ. J. Phys. Chem.*, 1996, **70**, No. 5 (Engl. Transl.)].
8. D. Nicolson and N. G. Parsonage, *Computer Simulation and the Statistical Mechanics of Adsorption*, Academic Press, New York, 1982.
9. E. N. Brodskaya and E. M. Piotrovskaya, *Rasplavy* [*Melts*], 1988, **2**, 29 (in Russian).
10. W. A. Steele, *Chem. Rev.*, 1993, **93**, 2355.
11. Yu. K. Tovbin, *Metod molekulyarnoi dinamiki v fizicheskoi khimii* [*Method of Molecular Dynamics in Physical Chemistry*], Nauka, Moscow, 1996, 128 (in Russian).
12. I. P. Prigogine, L. Mathot-Sarolea, and L. van Hove, *Trans. Faradey Soc.*, 1952, **48**, 485.
13. P. Cavalloti, *Surface Sci.*, 1979, **83**, 325.
14. Yu. K. Tovbin, *Zh. Fiz. Khim.*, 1998, **72**, 2280 [*Russ. J. Phys. Chem.*, 1998, **72**, No. 12 (Engl. Transl.)].
15. H. E. Stanley, *Introduction to Phase Transitions and Critical Phenomena*, Clarendon Press, Oxford, 1971.
16. L. Onsager, *Phys Rev.*, 1944, **65**, 117.
17. C. Domb, *Adv. Phys.*, 1960, **9**, 149; 245.
18. E. A. Guggenheim, *J. Chem. Phys.*, 1945, **13**, 253.
19. I. Prigogine, *The Molecular Theory of Solutions*, North-Holland Publ. Comp., Amsterdam, 1957.
20. N. A. Smirnova, *Molekulyarnaya teoriya rastvorov* [*The Molecular Theory of Solutions*], Khimiya, Leningrad, 1987, 360 pp. (in Russian).
21. J. O. Hirschfelder, C. F. Curtiss, and R. B. Bird, *Molecular Theory of Gases and Liquids*, Wiley, New York, 1954.
22. M. E. Fisher, *J. Math. Phys.*, 1963, **4**, 278.
23. Yu. K. Tovbin, *Dokl. Akad. Nauk SSSR*, 1981, **260**, 679 [*Dokl. Chem.*, 1981 (Engl. Transl.)].
24. Yu. K. Tovbin, *Dokl. Akad. Nauk SSSR*, 1990, **312**, 918 [*Dokl. Chem.*, 1990 (Engl. Transl.)].
25. E. V. Votyakov and Yu. K. Tovbin, *Zh. Fiz. Khim.*, 1993, **67**, 391 [*Russ. J. Phys. Chem.*, 1993, **67**, No. 2 (Engl. Transl.)].
26. Yu. K. Tovbin and E. V. Votyakov, *Physics of Low Dimensional Structures*, 1995, **10/11**, 105.
27. Yu. K. Tovbin and E. V. Votyakov, *Langmuir*, 1993, **9**, 2652.
28. E. V. Votyakov and Yu. K. Tovbin, *Zh. Fiz. Khim.*, 1994, **68**, 287 [*Russ. J. Phys. Chem.*, 1994, **68**, No. 2 (Engl. Transl.)].
29. E. V. Votyakov, Yu. K. Tovbin, J. M. D. MacElroy, and A. Roche, *Langmuir*, 1999, **15**, 5713.
30. A. M. Vishnyakov, E. M. Piotrovskaya, E. N. Brodskaya, E. V. Votyakov, and Yu. K. Tovbin, *Zh. Fiz. Khim.*, 2000, **74**, 501 [*Russ. J. Phys. Chem.*, 2000, **74**, No. 3 (Engl. Transl.)].
31. O. Yu. Batalin, Yu. K. Tovbin, and V. K. Fedyanin, *Zh. Fiz. Khim.*, 1980, **53**, 3020 [*Russ. J. Phys. Chem.*, 1980, **53**, No. 12 (Engl. Transl.)].
32. S. Sokolowski and J. Fischer, *Mol. Phys.*, 1990, **71**, 393.
33. M. E. Fisher and H. Nakanishi, *J. Chem. Phys.*, 1981, **75**, 5857.
34. H. Nakanishi and M. E. Fisher, *J. Chem. Phys.*, 1983, **78**, 3279.
35. P. Tarasona, U. M. B. Marconi, and R. Evans, *Mol. Phys.*, 1987, **60**, 573.
36. A. de Kreizer, T. Michalski, and G. H. Findenegg, *Pure Appl. Chem.*, 1991, **63**, 1495.
37. L. D. Gelb, K. E. Gubbins, R. Radhakrishnan, and M. Sliwinska-Bartkowiak, *Rep. Prog. Phys.*, 1999, **62**, 1573.
38. Yu. K. Tovbin and E. V. Votyakov, *Izv. Akad. Nauk, Ser. Khim.*, 2001, 48 [*Russ. Chem. Bull., Int. Ed.*, 2001, **50**, 50].

Received October 8, 2001;
in revised form March 25, 2002